Egyptian Journal of Neurosurgery

RESEARCH

Open Access

Angiographic analysis on posterior fossa hemorrhages and vascular malformations beyond aneurysms by CT angiography and digital subtraction angiography

S. Vignesh[1], Surya Nandan Prasad[1], Vivek Singh[1*], Zafar Neyaz[1], R. V. Phadke[1], Anant Mehrotra[2] and Prabhakar Mishra[3]

Abstract

Background: Posterior fossa malformations are less common than supratentorial malformations, but hemorrhages in posterior fossa are more serious due to presence of vital structures within this region. Most common cause of bleed in posterior fossa apart from hypertension is aneurysms but other vascular malformations are also there which cause hemorrhage. Here we discuss other causes of posterior fossa bleed beyond aneurysms.

Results: A total of 80 patients were evaluated: 47 (58.8%) had aneurysms, 29 (36.3%) had arteriovenous malformations, one each had developmental venous anomaly and brainstem cavernoma. Thirty vascular malformations were detected, of which 18 (62.1%) were pial arteriovenous malformations (AVMs), 11 (37.9%) were dural arteriovenous fistulas (dAVF), and one had developmental venous anomaly (DVA). Six patients of AVM underwent both DSA and CTA, and CTA could correctly diagnose only 2 of 4 pial AVMs detected by DSA. Among two dAVFs detected by DSA, CTA could demonstrate dAVF only in one patient.

Conclusion: CTA could be used as alternative to DSA in diagnosis and characterizing aneurysms in posterior fossa but for AVMs, 3D-CTA cannot replace DSA; however potential of time-resolved CTA (TR-CTA) appears promising.

Keywords: Posterior fossa bleed, AVM, Dural AVM, DSA

Background

Posterior fossa hemorrhages and vascular malformations are not so frequent as compared to that in anterior and middle cranial fossa. The various causes of posterior fossa hemorrhages include [1, 2] hypertension, trauma, aneurysms, arteriovenous malformations, blood dyscrasias, hemorrhage from tumors, amyloid angiopathy, sympathomimetic abuse and occasionally post-supratentorial surgery [3]. The narrow space of posterior fossa and the presence of many vital structures within this fossa lead to serious consequences in cases of bleeds. Immediate surgical treatment is needed for posterior fossa bleeds [4, 5]. To prevent mortality and morbidity, rapid diagnosis of the bleed and the underlying cause is of utmost importance.

The main imaging modalities for diagnosis include CT angiography (CTA) and digital subtraction angiography (DSA). Even though DSA is the gold standard for the diagnosis, CT angiography (CTA) with its recent technological advances has gained in importance on par with DSA. Some of the advantages of DSA include large field of view, high spatial resolution and temporal imaging capabilities, but it is time-consuming, invasive and associated with procedure-related complications [6, 7]. CTA

*Correspondence: singhvivek79@rediffmail.com
[1] Department of Radiodiagnosis, SGPGIMS, Lucknow, India
Full list of author information is available at the end of the article

is noninvasive, easy to perform and is well tolerated by patients with hemorrhage. Information on mural calcifications, luminal thrombi and proximity to bony structures of the skull base which are of surgical importance can be easily assessed with CTA. Technical parameters are very important for CTA. Concentration and dose of contrast agent, injection rate, and weight of the patient, hemodynamical factors and proper timing of the scan affect the quality of the imaging.

The purpose of the present study is to list and evaluate the various causes of posterior fossa hemorrhages with the angio-architectural determinants and to compare the diagnostic accuracy of CTA with DSA in detecting various posterior fossa vascular pathologies. In this study, we emphasize more on vascular malformations other than only aneurysms as cause of posterior fossa hemorrhage.

Methods

Patients

From January 2017–October 2018, 80 patients (49 males, 31 females) were included in our study. An informed written consent was taken from all patients. They had been admitted in our hospital with symptoms of non-traumatic posterior fossa hemorrhage or vascular pathologies. The mean age of the patients was 43.59 ± 1.584 (19–75 years). The diagnosis of the hemorrhage was made on non-contrast CT scan. Patients with posterior fossa SAH as a part of supratentorial pathology were excluded. Out of the total of 80 patients evaluated, 31 patients underwent both the procedures (CTA and DSA) within a mean interval of 6.2 ± 1.1 days.

Imaging protocol

CT angiography

CT angiography was performed on a 64-detector MDCT system (Brilliance; Philips medical systems, New Virginia, USA). The area covered was from C2 vertebra to the top of cranial vault, with the patient positioned supine and head immobilization achieved using adhesive strap. Non-ionic contrast medium (80–100 ml) was injected at a rate of 5 ml/s followed by saline flush of 40 ml using Medrad Stellant pressure injector. CT parameters were as follows: 0.75 s/r gantry rotation speed, 512×512 matrix, 0.6–0.9 pitch, 64×0.625 slice collimation, 220–240 mm field of view; 120 kVp tube voltage; 400 mA tube current. Data acquisition was started by monitoring contrast arrival in common carotid arteries using smart prep (bolus tracking method). The source images were transferred to dedicated work station—Extended Brilliance Work space (Koninklijke Philips electronics, Netherlands) for post-processing and image review. Apart from the source images, the methods utilized for better visualization included the multiplanar reformation (MPR), maximum intensity projection (MIP) and 3D volume rendering technique (VRT).

Digital subtraction angiography

DSA was carried out on Siemens Artis Zee Biplane or Philips Allura FD20 systems by two experienced interventional radiologists. Selective 4-vessel or 6-vessel DSA via femoral artery catheterization was performed. Anteroposterior, lateral, oblique and wherever necessary additional views of each vessel were obtained by manual injection of 60–80 ml nonionic contrast media. The images obtained were then reviewed in the dedicated work stations.

Image analysis

Two experienced radiologists who had >10 years' experience in field of neuroradiology analyzed the imaging independently, each being blinded to the other's readings and in particular, blinded to the findings obtained by the other modality. The main vessels evaluated were the V4 segment of the vertebral arteries (V4-VA), posterior inferior cerebellar arteries (PICAs), anterior inferior cerebellar arteries (AICAs), basilar artery (BA), superior cerebellar arteries (SCAs), straight sinus, transverse sinuses and sigmoid sinuses. The detected aneurysms were characterized based on its location, size, and incorporation of other arteries, calcification and intraluminal thrombi. The findings of arteriovenous malformations (AVMs) were characterized based on its location, nidus size, number of arterial feeders, dural feeders, venous drainage, cortical venous reflux and presence of nidal/feeding artery aneurysms.

Statistical analysis

The sensitivity, specificity and diagnostic accuracy of the CTA in detection of the posterior fossa hemorrhages and vascular malformations were compared with DSA. The comparison between the sizes of the aneurysms in two groups was made by using paired t test. The agreement between the two groups was made by using the appropriate nonparametric tests of significance. A p value < 0.05 was considered to be statistically significant. Statistical Package for Social Sciences version 21 (SPSS-21, IBM, Chicago, USA) was used for statistical analysis.

Results

A total of 80 patients were evaluated in this, of which 49 (61.3%) were males and 31 (39.8%) were females. The main presenting complaints with which the patients came were sudden onset headache followed with vomiting (75%). The other complaints were transient loss of consciousness seizures, vertigo and vision loss. Hemorrhage at presentation was present in 80% of the cases.

The hemorrhage was SAH (subarachnoid hemorrhage) with IVH (intraventricular hemorrhage) in 26 patients (32.5%), SAH without IVH in 23 patients (61%) and intraparenchymal in 14 patients (17.5%). Isolated intraventricular hemorrhage at presentation was noted in 3.8% of patients. In cases of SAH, according to the modified Fisher's grading, grade IV (thick SAH + IVH) was noted in 54%, grade III in 25%, grade II in 12.5% and grade I in 8.3%.

Out of the 80 patients evaluated, 47 (58.8%) patients had aneurysms, 29 (36.3%) had arteriovenous malformations, one patient had developmental venous anomaly, and one patient had brainstem cavernoma (Table 1). No cause could be detected in two patients. Among the 47 patients who had aneurysms, 24 (51.1%) were males and 23 (48.9%) were females. The age group ranged from 20 to 75 years with mean age of 46.96 ± 1.88 years. Among the 29 patients having AVMs, 21 (72.4%) were males and 8 (27.6%) were females. The age group ranged from 19 to 67 years with mean age of 36.24 ± 2.56 years. There was statistically significant difference between the age groups of aneurysms and AVM ($p < 0.05$, Kruskal–Wallis test). 70.2% of patients having aneurysms were > 40 years of age as compared to 69% of the patients having AVM were < 40 years of age. The two patients in whom no cause of hemorrhage could be detected were > 60 years of age. Both were hypertensive and likely cause of posterior fossa bleeds could be due to hypertension.

DSA detected 51 aneurysms in 47 patients ranging from 2 to 36 mm with mean size of 10.39 ± 1.12 mm. The smallest aneurysm detected was 2 mm.

Thirty vascular malformations were detected, of which 18 (62.1%) were pial arteriovenous malformations (AVMs), 11 (37.9%) were dural arteriovenous fistulas (dAVF), and one developmental venous anomaly (DVA). Most pial AVMs were located in cerebellum, while one pial AVM was located in the brainstem at the level of the pons. The mean nidus size in case of pial AVMs was 3.0 ± 1.55 cm. Among pial AVMs, 18 patients had arterial feeders from posterior circulation and only one patient had secondary meningeal feeder from anterior circulation (meningohypopyseal trunk of ICA). Among the dAVFs, 63.7% ($n = 7$) were present at the transverse-sigmoid junction, 27.3% ($n = 3$) were present at the torcula, and 9.1% (1) were present at the petrosal sinuses. The main feeders were from transosseous branches of occipital artery and posterior division of middle meningeal artery from ECA (12 patients), meningohypopyseal trunk from anterior circulation (9 patients) and dural branches of vertebral artery (6 patients). According to the Cognard classification [8], the most common type of dAVFs was type 2b and type 5 (Table 2). Out of 29 AVMs, 11 (37.9%) had associated aneurysms (AAs), of which 2 (6.9%) patients had one intranidal aneurysm, 5 (17.2%) had one feeding artery aneurysm, 3 (10.3%) had more than one feeding artery aneurysms, 1 (3.4%) patient had aneurysm in the draining vein, and 1 (3.4%) had both intranidal and feeder artery aneurysm. Most common location of feeder vessel aneurysm was in PICA ($n = 6$), followed by AICA ($n = 4$). The mean aneurysmal size in case of AA was 6.08 ± 0.67 mm.

Accuracy of CTA versus DSA

Of the 31 patients who underwent both the procedures, 23 patients (74.2%) had aneurysms, 4 patients (12.8%) had pial AVMs, 2 patients (6.5%) had dAVFs, and two patients (6.5%) had intraparenchymal hemorrhage which was negative on both CTA and DSA. The interval between the two procedures in patients having aneurysms was 4.5 ± 0.9 (0–14 days), and those having AVMs were 13.7 ± 2.9 (4–23 days).

Sensitivity and specificity of CTA in detecting aneurysms in posterior fossa are high, and no statistically significant difference between the sizes of the aneurysms and its detection was found between CTA and DSA ($p > 0.05$, Paired t test). CTA in addition showed the presence of mural calcifications and luminal thrombus which were not seen on DSA.

In case of vascular malformations, CTA could correctly diagnose only 2 of the 4 pial AVMs detected by the DSA. The cause of hemorrhage on CTA was found to be aneurysms in right SCA and left PICA in the two cases of pial AVMs. Among the 2 dural AVFs detected by DSA, CTA could demonstrate the dAVF only in one patient. In the other patient, the presence of calcifications in left transverse sinus, enlarged spinal perimedullary veins and enlarged occipital arteries pointed towards the possibility of dAVF, even though there was no detectable communication between the arterial and venous system. CTA correctly detected 22/24 arterial

Table 1 Causes of posterior fossa hemorrhage and vascular malformation according to sex

	Aneurysm	AVM	DVA	Cavernoma	Negative	Total
Male	24	21	1	1	2	49
Female	23	8	0	0	0	31
Total	47	29	1	1	2	80

Table 2 Characteristics of AVM and dAVF in our study

AVM and AVF characteristics	DSA
Pial AVMs diagnosed	
Total	18
Cerebellum	17 (94.4)
Brainstem	1 (5.5)
Size of nidus	
< 3 cm	10 (55.6)
3–6 cm	7 (38.9)
> 6 cm	1 (5.6)
Total no. of arterial feeders	
Posterior circulation	30
Anterior circulation	1
Dural supply	0
Intranidal aneurysm	3 (16.7)
Flow-related aneurysms	
Total	19 (50)
Feeder vessel	18 (44.4)
Draining vein	1 (5.6)
Dural AVFs diagnosed	
Total	11
Transverse-sigmoid junction	7 (63.7)
Torcular	3 (27.3)
Petrosal	1 (9.1)
Cognard classification [8]	
I—Antegrade sinusoidal flow	2 (18.2)
IIa—Reflux sinusoidal	0 (0)
IIb—Reflux sinusoidal	3 (27.3)
III—Direct shunt into cortical vein	1 (9.1)
IV—As III with venous ectasia	1 (9.1)
V—Perimedullary venous drainage	4 (36.4)
Total no. of ECA feeders	27
No. of other arterial feeders	
Posterior circulation	9
Anterior circulation	12

feeders. The missed arterial feeders were dural feeders from middle meningeal and occipital artery. The sensitivity of CTA in correctly diagnosing AVM as the cause of the hemorrhage was found out to be only 66.7%, but the specificity was 100% (Table 3).

The overall sensitivity and specificity of CTA in detecting the posterior fossa hemorrhage and vascular malformations as compared to DSA are 96.6% and 100%, respectively (Table 3). The positive and negative predictive values are 100% and 75%, respectively. There was good measure of agreement between CTA and DSA in detecting the cause ($\kappa = 0.76 \pm 0.13$; $p < 0.05$).

Discussion

The posterior fossa bleeds and vascular pathologies are associated with increased morbidity and mortality, and this necessitates their rapid and correct diagnosis. The ideal imaging modality should be fast to perform, minimally invasive, reproducible and associated with minimal complications. Apart from all these, the imaging modality must be able to correctly identify the cause of hemorrhage along with their angio-architectural characteristics. In case of aneurysms, it must be able to accurately localize the aneurysm and provide details about surrounding vascular anatomy, presence of associated calcifications and intraluminal thrombus, which all would help in deciding the appropriate treatment plan. And in case of arteriovenous malformations, the number of arterial feeders, presence or absence of dural feeders, type of venous drainage, and more importantly the presence of associated aneurysms and their characterization are of prime importance. CT angiography with its recent advances has gained in importance on par with conventional catheter-based angiography.

The most common cause of nontraumatic subarachnoid hemorrhage is aneurysms [1]. They usually present with sudden onset headache. This is in accordance with our data, in which 58% of the patients presenting with SAH had aneurysms. AVMs usually present in young adults as spontaneous intracranial intraparenchymal hemorrhage more commonly than SAH [1]. In our study, 69% of the AVMs occurred in < 40 years of age and 70% of aneurysms were in > 40 years of age. Intraparenchymal hemorrhage was present in 41% of the AVM patients. The most common cause of posterior fossa bleeds in elderly is hypertension [2], which was seen only in 2.5%

Table 3 Diagnostic efficacy of CTA compared to DSA (gold standard)

	Sensitivity (%)	Specificity (%)	Positive predictive value (%)	Negative predictive value (%)	Diagnostic accuracy (%)
Per aneurysm basis	96	–	100	–	96
Per patient basis for detection of aneurysms	95.7	100	100	90	96.9
Per patient basis for detection of AVMs	66.7	100	100	92.9	93.8
overall	96.6	100	100	75	96.9

of our study which can be attributed to the fact that the elderly patients presenting with bleeds and who were known hypertensives were not taken up for angiographic evaluation.

The most common site of the aneurysm in the posterior fossa is the vertebral arteries, accounting for 37% of the cases in the posterior fossa. Among the cerebellar arteries, the most common artery is PICA (25.5%) (Fig. 1a–c). The most common site of pial AVMs is cerebellum in our study (Fig. 2a, b) and, among dural AVFs, the transverse-sigmoid junction. The main feeder supplying the posterior fossa AVMs and dAVFs apart from posterior circulation arteries is the meningohypopyseal trunk (branch of cavernous segment of ICA) (Fig. 3a, b). And as the dAVFs in the posterior fossa are close to the skull base, they mostly recruit the transosseous and dural branches of the ECA, especially occipital arteries and the posterior division of middle meningeal artery(Figs. 4 and 5).

A number of research studies have been performed to evaluate the multidetector CT angiography for the evaluation of aneurysms and vascular malformations. Most studies have worked on detecting aneurysms in posterior fossa via CTA [9–12] and have found high sensitivity and specificity for detecting large size aneurysm which is equal to that of DSA.

The low sensitivity of the CTA in detecting smaller sized aneurysms can be attributed partially to the lower spatial resolution of the CT compared to the DSA. Various post-processing techniques have been developed to

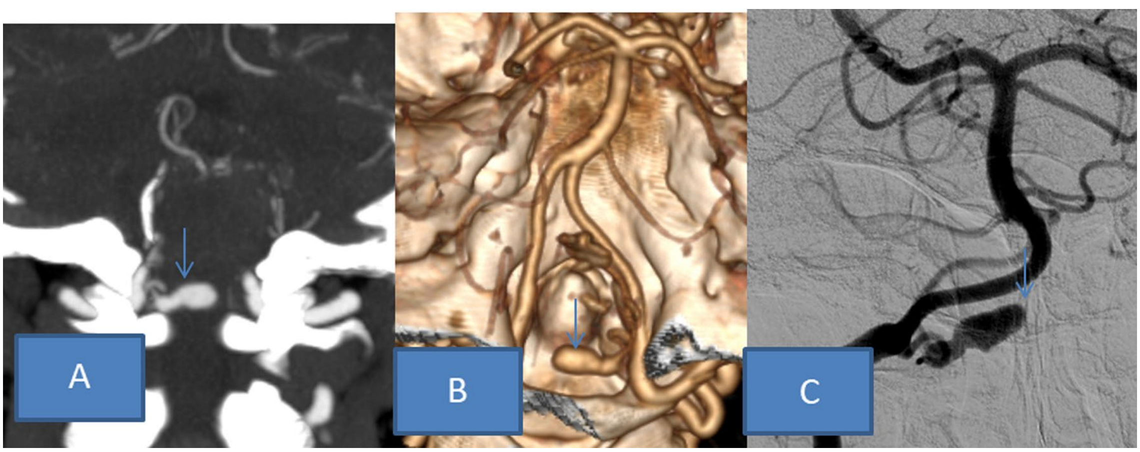

Fig. 1 Right posterior inferior cerebellar artery (PICA) aneurysm; **a** Coronal MIP image, **b** volume reconstructed image (VRI), **c** DSA image in AP view, of the same patient showing aneurysm in the proximal part of PICA just after its origin (arrow pointing towards aneurysm)

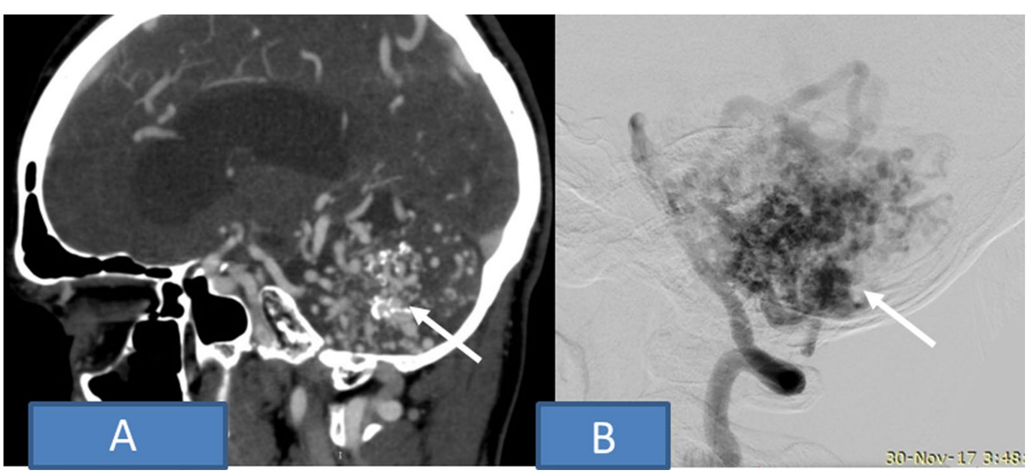

Fig. 2 Pial AVM; **a** Sagittal MIP image, and **b** DSA image in lateral view in the same patient showing pial AVM in the posterior fossa with tangle of vascular channels—nidus (white arrows)—with enlarged draining veins

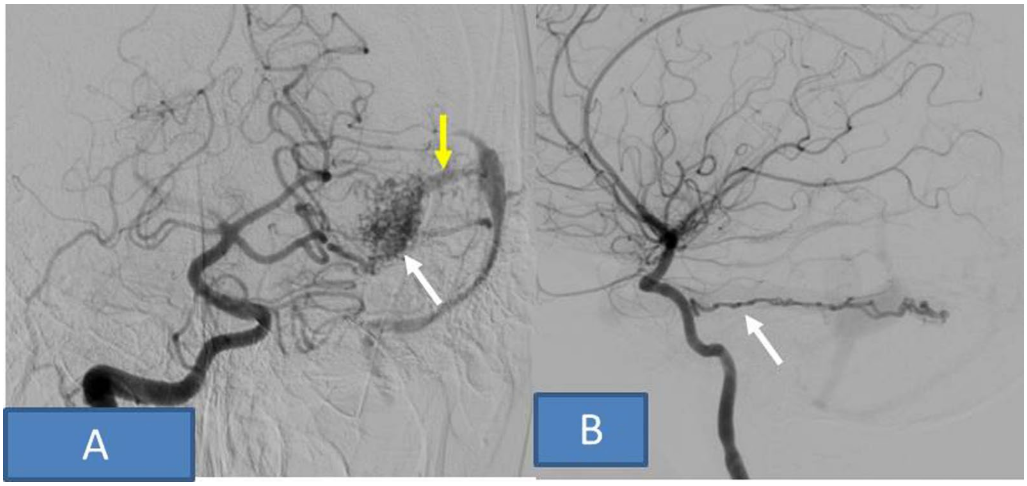

Fig. 3 Pial AVM; **a** DSA image in AP view showing pial AVM in the posterior fossa with arterial feeder from dilated SCA (white arrow) and drainage via early draining vein (yellow arrow) into the left transverse/sigmoid sinus, **b** DSA image in lateral view showing dilated meningohypopyseal trunk (white arrow) supplying the AVM

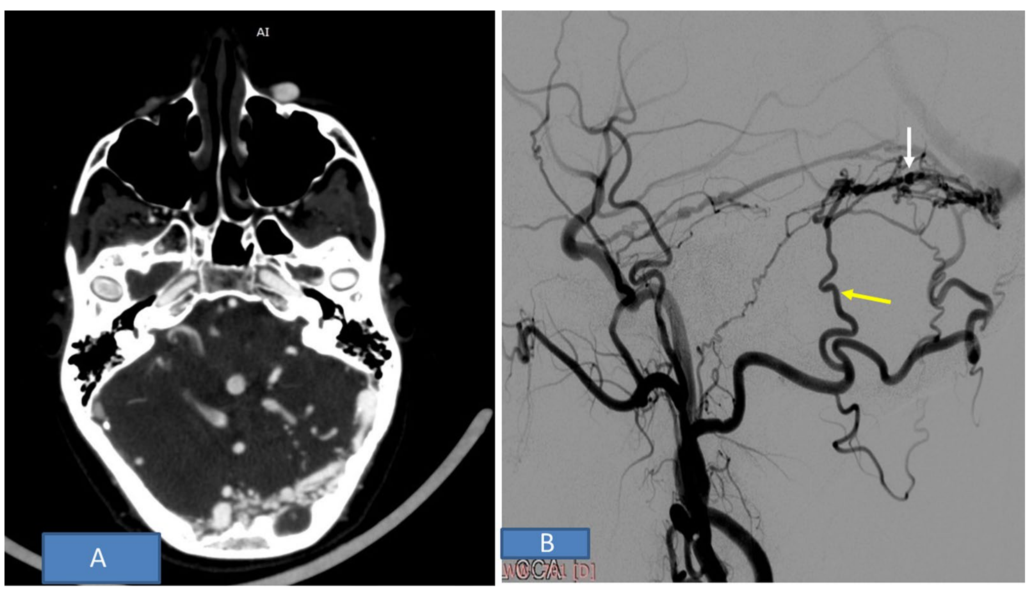

Fig. 4 Dural arteriovenous fistula (dAVF); **a** Axial MIP image showing the calcifications in torcula and increased vascular channels within the left transverse sinus, **b** DSA image in lateral view of the same patient showing dAVF (Type 1) in the torcular region (white arrow) with feeders from occipital artery (yellow arrow)

increase spatial resolution of CTA which allows better aneurysm visualization [13, 14].

The main advantage of CTA is that it is superior to DSA in detection of calcifications and thrombus [15], which plays an important role in deciding the treatment plan. 3D-CTA has the added advantage of able to reconstruct the image in any desired plane or angle using the VRI (volume rendered imaging) technique. Conventional DSA can provide only two-dimensional images; hence various projections needed to be taken in order to delineate the surrounding vascular anatomy. Similar to 3D-CTA, 3D-DSA has been introduced in recent times, which can reconstruct the image in any chosen projection [16, 17].

There are very few studies where other causes of posterior fossa bleed other than aneurysms were evaluated.

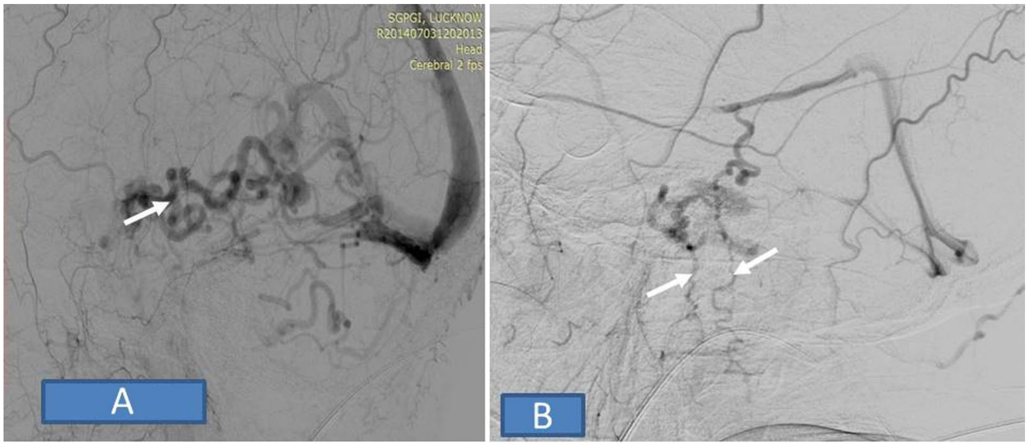

Fig. 5 dAVF—Cognard classification; **a** Type IIb—showing cortical venous reflux (white arrow), **b** Type V—spinal perimedullary venous drainage (white arrows)

CTA has low sensitivity in detecting the AVMs/AVFs [18, 19]. In our study, the sensitivity of CTA in diagnosing the AVMs was only 66.7%. Among the detection of arterial feeders, CTA has good sensitivity of 92%, but in specifically detecting the dural feeders, the sensitivity of CTA is only 66%. The detection of transosseous feeders still remains a challenge with CTA. The main reason for the low sensitivity with CTA is their lack of information regarding the flow (dynamic information) because of their one-time acquisitions and only one phase of the flow dynamics. The lack of clear demonstration of early venous drainage leads to difficulty in diagnosing the AVMs. Technological advancements in computed tomography (CT) now permit dynamic imaging techniques of the whole brain. Such time-resolved or four-dimensional computed tomography angiography (TR-CTA/4D-CTA) can be used to evaluate the hemodynamics, in addition to the morphology [20, 21].

Posterior fossa AVMs have been reported to be an independent predictor of increased morbidity and mortality. This may be due to frequent presentation of posterior fossa AVMs with hemorrhage and increased association of the associated aneurysms with posterior fossa AVMs as compared to supratentorial AVMs [22, 23]. The incidence of aneurysms associated with AVMs has been reported to be around 2.7–21% [24]. Klaus-Peter Stein et al. [25] reported that hemorrhage was associated with 86% of the infratentorial AVMs as compared to only 36% of the supratentorial AVMs. The aneurysms were associated with 29% of the cases in case of posterior fossa, compared to 14% in supratentorial AVMs. Twenty-nine AVMs were obtained in our study in posterior fossa of which 37.9% had aneurysms and 10.3% had more than one feeding artery aneurysms. (Fig. 6a, b).

Rare cause of intracranial bleed is developmental venous anomaly which was detected in one of our case (Fig. 7) where no associated AVM or aneurysm could be detected. The main limitation in our study was the unavoidable selection bias in which older patients with spontaneous intraparenchymal hemorrhage were not taken up for the study due to their health conditions. The smaller sample size might also explain the lower sensitivity of CTA in detecting the AVMs/dAVFs.

Conclusion

In conclusion, CTA is a simple, fast and noninvasive imaging modality that can be used to detect and characterize the vascular pathologies in posterior fossa. The overall sensitivity of CTA in detecting the cause of hemorrhage in posterior fossa is 96.6% with diagnostic accuracy of 96.9%. However sensitivity of CTA in diagnosing the AVMs was only 66.7%, and for detection of arterial feeders, CTA has good sensitivity of 92%, but specifically in detecting the dural feeders, the sensitivity of CTA is only 66%. The detection of transosseous feeders still remains a challenge with CTA. Overall CTA can be used in the initial investigation for posterior fossa hemorrhages. CTA could be used as an alternative to DSA in the diagnosis and characterization of aneurysms in posterior fossa and for treatment planning. For the characterization of posterior fossa AVMs, the 3D-CTA cannot replace DSA; however, the potential of time-resolved CTA (TR-CTA) appears promising.

Fig. 6 Associated Aneurysms in AVM; **a** DSA image showing intranidal aneurysm (white arrow), **b** DSA image showing feeder vessel aneurysm in PICA (white arrow) supplying the AVM in the posterior fossa (yellow arrow)

Fig. 7 Developmental venous anomaly (DVA) or venous angioma; DSA image in AP view showing 'medusa head' appearance (white arrow) of medullary veins with early dilated draining vein into torcula

Abbreviations
CTA: Computed tomography angiography; DSA: Digital subtraction angiography; AVM: Arteriovenous malformation; dAVF: Dural arteriovenous fistula; MRI: Magnetic resonance imaging; TR-CTA: Time-resolved CT angiography; ICA: Internal carotid artery; ECA: External carotid artery; PCA: Posterior cerebral artery; PICA: Posterior inferior cerebellar artery; AICA: Anterior inferior cerebellar artery; SCA: Superior cerebellar artery.

Acknowledgements
Department of Neurosurgery and Neurology, SGPGIMS, Lucknow. India.

Authors' contributions
SV, SNP, VS and RVP were responsible for the data acquisition and analysis. Manuscript preparation and editing was primarily done by SV, VS and ZN. Intellectual content and patient management was done by VS and AM. Statistical analysis was done by PM. All authors read and approved the final manuscript.

Funding
None.

Availability of data and materials
Yes.

Declarations

Ethics approval and consent to participate
Yes obtained by the institutional ethics committee via IEC code -2017-91-MD-EXP, dated 3/5/2017. An written informed consent was taken from all patients.

Consent for publication
Not applicable.

Competing interests
The authors declare that they have no competing interests.

Author details
[1]Department of Radiodiagnosis, SGPGIMS, Lucknow, India. [2]Neurosurgery, SGPGIMS, Lucknow, India. [3]Biostatistics Department, SGPGIMS, Lucknow, India.

Received: 10 June 2021 Accepted: 7 March 2022
Published online: 18 April 2022

References

1. Osborn AG. Osborn's brain—imaging, pathology and anatomy. 2nd ed. Sal Lake City, UT: Elsevier, Inc.; 2017. Section 2, Nontraumatic hemorrhage and vascular lesions; p. 103–97.
2. Dayes LA, Purtzer TJ, Shahhal I, Cojocaru T, Knierim D, Soloniuk D. Acute spontaneous cerebellar hemorrhage. J Natl Med Assoc. 1986;78(6):495–9.
3. Cloft HJ, Matsumoto JA, Lanzino G, Cail WS. Posterior fossa hemorrhage after supratentorial surgery. AJNR Am J Neuroradiol. 1997;18(8):1573–80.
4. Neacsu A, Ciurea AV. General considerations on posterior fossa arteriovenous malformations (clinics, imaging and therapy). Actual concepts and literature review. J Med Life. 2010;3(1):26–35.
5. Han J, Lee HK, Cho TG, Moon JG, Kim CH. Management and outcome of spontaneous cerebellar hemorrhage. J Cerebrovasc Endovasc Neurosurg. 2015;17(3):185–93.
6. Klingebeil R, Kentenich M, Bauknecht HC, Masuhr F. Comparative evaluation of 64-slice CT angiography and digital subtraction angiography in assessing cervico-cranial vasculature. Vasc Health Risk Manag. 2008;4:901–3.
7. Leffers AM, Wagner A. Neurologic complications of cerebral angiography. A retrospective study of complication rate and patient risk factors. Acta Radiol. 2000;41(3):204–10.
8. Cognard C, Gobin YP, Pierot L, Bailly AL, Houdart E, Casasco A, et al. Cerebral dural arteriovenous fistulas: clinical and angiographic correlation with a revised classification of venous drainage. Radiology. 1995;194:671–80.
9. Donmez H, Serifov E, Kahriman G, Mavili E, Durak AC, Menkü A. Comparison of 16-row multislice CT angiography with conventional angiography for detection and evaluation of intracranial aneurysms. Eur J Radiol. 2011;80(2):455–61.
10. Li Q, Lv F, Yao G, Li Y, Xie P. 64-section multidetector CT angiography for evaluation of intracranial aneurysms: comparison with 3D rotational angiography. Acta Radiol. 2014;55(7):840–6.
11. Wang H, Li W, He H, Luo L, Chen C, Guo Y. 320-detector row CT angiography for detection and evaluation of intracranial aneurysms: comparison with conventional digital subtraction angiography. Clin Radiol. 2013;68(1):e15-20.
12. Milošević Medenica S, Vućković V, V, Prstojević B,. 64-slice CT angiography in the detection of intracranial aneurysms: comparison with DSA and surgical findings. Neuroradiol J. 2010;23(1):55–61.
13. Sakamoto S, Kiura Y, Shibukawa M, Ohba S, Arita K, Kurisu K. Subtracted 3D CT angiography for evaluation of internal carotid artery aneurysms: comparison with conventional digital subtraction angiography. AJNR Am J Neuroradiol. 2006;27(6):1332–7.
14. Luo Z, Wang D, Sun X, Zhang T, Liu F, Dong D, Chan NK, Shen B. Comparison of the accuracy of subtraction CT angiography performed on 320-detector row volume CT with conventional CT angiography for diagnosis of intracranial aneurysms. Eur J Radiol. 2012;81(1):118–22.
15. Kokkinis C, Vlychou M, Zavras GM, Hadjigeorgiou GM, Papadimitriou A, Fezoulidis IV. The role of 3D-computed tomography angiography (3D-CTA) in investigation of spontaneous subarachnoid haemorrhage: comparison with digital subtraction angiography (DSA) and surgical findings. Br J Neurosurg. 2008;22(1):71–8.
16. Wong SC, Nawawi O, Ramli N, Abd Kadir KA. Benefits of 3D rotational DSA compared with 2D DSA in the evaluation of intracranial aneurysm. Acad Radiol. 2012;19(6):701–7.
17. Sugahara T, Korogi Y, Nakashima K, Hamatake S, Honda S, Takahashi M. Comparison of 2D and 3D digital subtraction angiography in evaluation of intracranial aneurysms. AJNR Am J Neuroradiol. 2002;23(9):1545–52.
18. Biswas S, Chandran A, Radon M, Puthuran M, Bhojak M, Nahser HC, Das K. Accuracy of four-dimensional CT angiography in detection and characterisation of arteriovenous malformations and dural arteriovenous fistulas. Neuroradiol J. 2015;28(4):376–84.
19. Singh R, Gupta V, Ahuja C, Kumar A, Mukherjee KK, Khandelwal N. Role of time-resolved-CTA in intracranial arteriovenous malformation evaluation at 128-slice CT in comparison with digital subtraction angiography. Neuroradiol J. 2018;31(3):235–43.
20. Wang H, Ye X, Gao X, Zhou S, Lin Z. The diagnosis of arteriovenous malformations by 4D-CTA: a clinical study. J Neuroradiol. 2014;41(2):117–23.
21. Taschner CA, Gieseke J, Le Thuc V, Rachdi H, Reyns N, Gauvrit JY, Leclerc X. Intracranial arteriovenous malformation: time-resolved contrast-enhanced MR angiography with combination of parallel imaging, keyhole acquisition, and k-space sampling techniques at 1.5 T. Radiology. 2008;246(3):871–9.
22. Torné R, Rodríguez-Hernández A, Arikan F, Romero-Chala F, Cicuéndez M, Vilalta J, Sahuquillo J. Posterior fossa arteriovenous malformations: significance of higher incidence of bleeding and hydrocephalus. Clin Neurol Neurosurg. 2015;134:37–43.
23. Arnaout OM, Gross BA, Eddleman CS, Bendok BR, Getch CC, Batjer HH. Posterior fossa arteriovenous malformations. Neurosurg Focus. 2009;26(5):E12.
24. Stapf C, Mohr JP, Pile-Spellman J, Sciacca RR, Hartmann A, Schumacher HC, Mast H. Concurrent arterial aneurysms in brain arteriovenous malformations with haemorrhagic presentation. J Neurol Neurosurg Psychiatry. 2002;73(3):294–8.
25. Stein KP, Wanke I, Forsting M, Oezkan N, Huetter BO, Sandalcioglu IE, Sure U. Associated aneurysms in infratentorial arteriovenous malformations: role of aneurysm size and comparison with supratentorial lesions. Cerebrovasc Dis. 2016;41(5–6):219–25.

Publisher's Note